Dalton Transactions

# Barium and Titanium Dithiocarbamates as Precursors for Colloidal Nanocrystals of Emerging Optoelectronic Materials



| | |
|---|---|
| Journal: | *Dalton Transactions* |
| Manuscript ID | DT-COM-09-2021-003018.R1 |
| Article Type: | Communication |
| Date Submitted by the Author: | 29-Sep-2021 |
| Complete List of Authors: | Ingram, Nicole; Mississippi State University, Chemistry<br>Jordan, Brian; Mississippi State University, Chemistry<br>Donnadieu, Bruno; Mississippi State University, Chemistry<br>Creutz, Sidney; Mississippi State University, Chemistry |
| | |

COMMUNICATION

# Barium and Titanium Dithiocarbamates as Precursors for Colloidal Nanocrystals of Emerging Optoelectronic Materials

Nicole E. Ingram,[a] Brian J. Jordan,[a] Bruno Donnadieu,[a] Sidney E. Creutz[a*]

Received 00th January 20xx,
Accepted 00th January 20xx

DOI: 10.1039/x0xx00000x

**The synthesis and structures of N,N-dialkyldithiocarbamate complexes of barium are reported; the compounds crystallize as one-dimensional coordination polymers. In combination with a titanium dithiocarbamate precursor, the compounds are demonstrated as competent single-source precursors for the solution-based preparation of colloidal $BaTiS_3$ nanorods.**

Alkaline earth metal sulfides have been of interest for optoelectronic applications for decades, especially as hosts for luminescent dopants. Recent interest in novel and emerging low- and mid-bandgap semiconductors for a range of applications, especially as potential photovoltaic absorbers, has drawn specific attention to a class of alkaline earth metal-group 4 transition metal ternary chalcogenides with general formula $(AE)M^{IV}S_3$.[1] This group includes materials with a distorted perovskite structure such as $BaZrS_3$ (Figure 1), which have been predicted, on the basis of their optical properties, to rival the efficiency of the lead halide perovskites in photovoltaic applications. Other $(AE)M^{IV}S_2$ materials that adopt a non-perovskite, hexagonal needle-like phase, such as $BaTiS_3$ and $SrTiS_3$, have also shown intriguing and potentially useful properties in terms of optical anisotropy, mid-IR birefringence, and thermal transport (Figure 1).[2–4] However, synthetic methods to access these materials are limited and generally require very high temperatures (Figure 1a-b),[2,5] making them incompatible with most thin-film solution-processing techniques.

There is currently only one report of the solution synthesis of $(AE)M^{IV}S_3$ nanomaterials (Figure 1c),[6] and the development of new synthetic approaches is a pressing avenue of current research.[7] In this prior report, reactive titanium and barium amides were combined with N,N'-diethylthiourea in oleylamine to give $BaTiS_3$ nanorods. An alternative approach to $(AE)M^{IV}S_3$ materials would be to use sulfur-ligated $Ba^{2+}$ and $M^{4+}$ (M = $Ti^{4+}$, $Zr^{4+}$, $Hf^{4+}$) complexes as "single-source precursors", obviating the need for an exogenous sulfur source. Here, we provide proof of principle for this approach through (1) the synthesis and characterization of new barium dithiocarbamate complexes, followed by (2) their application, in combination with a titanium dithiocarbamate precursor, in the solution-phase synthesis of $BaTiS_3$ nanoparticles.

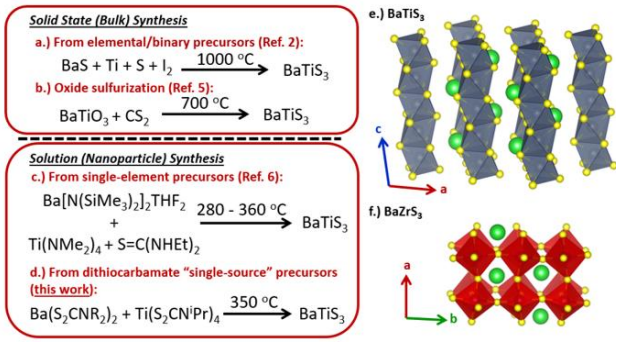


**Figure 1.** (a-d) Synthetic approaches to $BaTiS_3$ in the bulk and as nanocrystals. (e.) Structure of hexagonal $BaTiS_3$. (f.) Structure of $BaZrS_3$, an example of a chalcogenide perovskite.

Metal dithiocarbamate complexes have found widespread application as "single-source precursors" (SSPs) for the preparation of metal chalcogenide materials, especially thin films (*via* chemical vapor deposition) and nanomaterials (typically *via* thermal decomposition in solution).[8] This approach has been applied widely to transition metal sulfides, *p*-block chalcogenides such as PbS and $Bi_2S_3$, and to a lesser extent to *s*-block chalcogenides, in particular CaS and SrS.[9–11] Applications of metal dithiocarbamates to nanocrystal synthesis have also been extended to ternary and quaternary sulfide materials.[8] It is noteworthy that there are no prior reports of the use of group 4 (titanium, zirconium, or hafnium) dithiocarbamate complexes as precursors for the solution synthesis of sulfide nanomaterials; their use in the preparation of thin films by CVD has been reported in a thesis.[8,12]

[a] *Department of Chemistry, Mississippi State University, Mississippi State, MS 39762, USA. E-mail: screutz@chemistry.msstate.edu*
† These authors contributed equally.
Electronic Supplementary Information (ESI) available: Detailed synthetic procedures, characterization data for compounds and nanoparticles, additional experimental data. See DOI: 10.1039/x0xx00000x

Well-characterized examples of barium complexes of chalcogenide (S or Se) donor ligands are somewhat rare. In general, sulfur-coordinated barium ions are also supported by multiple additional ancillary ligands or solvent, which typically coordinate through an oxygen donor. Notable examples of such compounds include monomeric $Ba(THF)_4(SAr_2)_2$ compounds synthesized using bulky arenethiolates,[13] barium complexes of mercaptopyridine or methimazolyl scorpionate ligands and of a chelating dithioimidodiphosphinate ligand,[14,15] a tetrabarium cluster supported by tetrathiosquarate ligands,[16] and a polymeric barium dithiocarbonato complex containing barium ions with a $BaO_2S_7$ coordination environment.[17] Only one crystallographically characterized example of a coordination complex containing a barium ion with an all-sulfur coordination environment has been reported, within a hexabarium-$\mu_6$-sulfido cluster supported by *t*-butylthiolate ligands and coordinated methylpyrrolidinone solvent, which was reported to have crystallized fortuitously over the course of six years in an NMR tube.[18]

There is also limited prior literature on barium complexes involving dithiocarbamate ligands. Well-characterized examples are limited to complexes of amino acid-derived dithiocarbamates, where barium coordinates both to the sulfur atom(s) of the dithiocarbamate moiety and the oxygen atoms of the amino acid-derived carboxylate group.[19] Only one example of such a barium dithiocarbamate complex, barium *N*-dithiocarboxylatoglycinate trihydrate, has been crystallographically characterized; here, the coordination sphere of the barium ion consists of two sulfur atoms from the dithiocarbamate ligand and seven oxygen atoms (four from solvent water).[20] These barium dithiocarbamate compounds have been applied primarily as transmetallating agents for the preparation of amino acid-derived dithiocarbamate complexes of transition metals.[21–24] Two very recent reports describe the use of barium N,N-diethyldithiocarbamate and barium N,N-diisopropyldithiocarbamate precursors for the preparation of $Ba^{2+}$-doped silver sulfide and iron sulfide films, respectively, by physical vapor deposition, although the proposed precursor complexes were characterized only by infrared spectroscopy.[25,26]

Here, as a step in our effort to test the utility of dithiocarbamates as single-source precursors in the synthesis of $(AE)M^{IV}S_3$ materials, we have synthesized and characterized four examples of barium dithiocarbamate complexes, $Ba(S_2CNR_2)_2$, bearing different alkyl substituents, two of which have been crystallographically characterized (*vide infra*).

Barium dithiocarbamate compounds **1-4** bearing N,N-disubstituted dithiocarbamate ligands with either primary or secondary alkyl substituents were synthesized based on a protocol adapted from the previously reported synthesis of calcium and strontium N,N-diiospropyldithiocarbamates as shown in Scheme 1.[27,9] Initial formation of dithiocarbamate anions *in situ* in water or water/ethanol mixtures is followed by the addition of metallic barium to the reaction mixture, leading to the formation of the desired complexes, which can be recrystallized finally from ether/tetrahydrofuran mixtures. Detailed procedures for each ligand are provided in the Supporting Information. Notably, despite the fact that the reaction is carried out in water or water/ethanol mixtures, formally anhydrous barium dithiocarbamate complexes are accessed readily following recrystallization (compounds are also dried *in vacuo* at 80 °C for twelve hours before use in nanocrystal synthesis). The use of water-free precursors is likely important for the success of the subsequent nanocrystal synthesis reactions (*vide infra*).

The barium dithiocarbamate complexes are soluble or partially soluble in polar coordinating solvents (including ethanol, methanol, and tetrahydrofuran) and insoluble in nonpolar or noncoordinating solvents such as chloroform and dichloromethane. While the compounds most likely exist in solution as solvates, they crystallize in the solid state as one-dimensional coordination polymers. Thin, needle-like crystals of compounds **1** and **2** were grown from THF/diethyl ether, and the structures of these complexes have been determined by single-crystal X-ray diffraction. Both complexes crystallize in the solid state with each pair of neighbouring barium ions bridged by two dithiocarbamate ligands (Figure 2; further discussion below). Complex **3** gives rise to needle-like crystals similar in appearance to **1** and **2** upon recrystallization from THF/ether; however, crystals of **3** diffracted poorly, and a satisfactory structural solution and refinement could not be obtained after several attempts. We were unable to grow X-ray quality crystals of complex **4**.

**Scheme 1**. Synthesis of barium dithiocarbamate precursors.

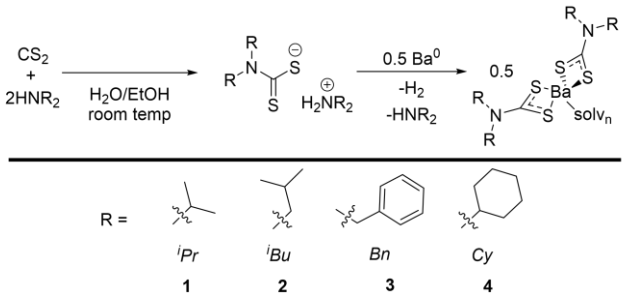


In the structure of compound **1** (Figure 2A), the asymmetric unit includes three $Ba^{2+}$ ions, two of which are eight-coordinate with an all-sulfur coordination environment in a distorted square antiprismatic geometry, while the third is additionally coordinated to two THF molecules and is ten-coordinate. This results in a one-dimensional coordination polymer with a kinked chain, as illustrated in Figure 2A. In contrast, in the structure of compound **2**, which bears longer-chain diisobutyl substituents, all barium ions are coordinated only by sulfur donors from the dithiocarbamate ligands in distorted square antiprismatic environments, resulting in a linear chain with each dithiocarbamate donor bridged between two neighboring barium ions (Figure 2B). Structural differences between the two compounds may be the result of the higher degree of steric hindrance engendered by the isopropyl substituents in the immediate vicinity of the $Ba^{2+}$ ion relative to the isobutyls.

Magnified depictions of the environment around the ten-coordinate $Ba^{2+}$ ion in **1** and around one of the eight-coordinate $Ba^{2+}$ ions (shown for compound **2**; the geometry around the eight-coordinate ions in **1** is similar) are also depicted in Figure 2C-D; steric crowding around the ten-coordinate $Ba^{2+}$ ion may be responsible for the longer and more variable Ba-S bond lengths (~3.3 to 3.5 Å), whereas the Ba-S bond lengths in the eight-coordinate ions are all close to 3.2 Å.

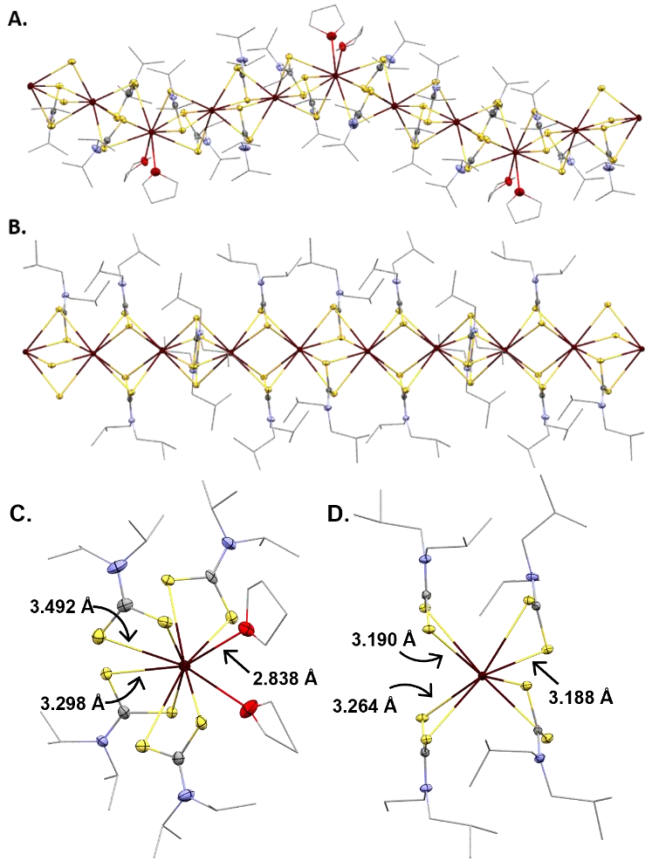


**Figure 2.** Crystal structures of barium dithiocarbamate complexes **1** (A) and **2** (B). Hydrogen atoms are omitted and, for clarity, carbons in alkyl groups are represented in wireframe. Other atoms are shown as thermal ellipsoids at 50% probability. Both structures are truncated sections of one-dimensional coordination polymers. Panels (C) and (D) show magnified views of the coordination environments around the 10-coordinate $Ba^{2+}$ ion in **1** (C) and one of the 8-coordinate $Ba^{2+}$ ions in **2** (D), along with selected bond distances. (Red = O; yellow = S; maroon = Ba; purple = N; gray = C).

Compound **4** (R = Cy) shows qualitatively lower solubility than the other members of this series, dissolving sparingly in THF, methanol, or DMSO, while compounds **1**, **2**, and **3** are highly soluble. It should, however, be noted that compounds **1** and **4** were observed to decompose slowly in methanol solution at room temperature, giving rise over the course of several days to free amine and an unidentified, insoluble white precipitate. All compounds were characterized by NMR in $d_4$-methanol or $d_6$-DMSO solution. NMR analysis indicates that coordinated solvent is removed from the compounds by drying *in vacuo* at 80 °C, as no additional solvent is observed in the NMR of the as-synthesized and dried compounds; some THF is observed in solution when crystals of compound **1** are analyzed by NMR following only brief vacuum drying at room temperature. The structure of the compounds in solution is not known with certainty, although it is likely that the solvent ($CD_3OD$ or DMSO) coordinates to the barium ions in order to break up the solid-state coordination polymer. While compounds **2** and **3** show a single set of sharp resonances in the $^1H$ NMR, suggesting that all dithiocarbamate ligands and substituents are equivalent on the NMR timescale, compounds **1** and **4** show broadened NMR features and two sets of resonances consistent with slow rotation of the C-N bonds of the isopropyl (**1**) or cyclohexyl (**4**) groups on the NMR timescale. Similar behavior has been previously observed in diisopropyldithiocarbamate complexes of $Sr^{2+}$ and other metals, and the kinetics and mechanism of this process have been studied in detail in prior reports.[27–29] At low temperature (243 K), the resonances sharpen, clearly showing two chemically inequivalent environments for the substituents (see Supporting Information for further discussion).

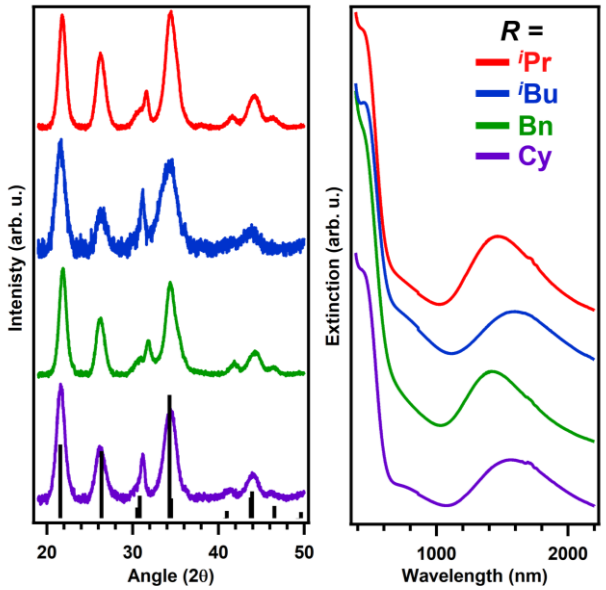


**Figure 3.** Characterization of $BaTiS_3$ nanocrystals synthesized using the standard conditions described in the text with barium dithiocarbamate precursors $Ba(S_2CNR_2)_2$ with different substituents (R). **(Left)** Powder X-ray diffraction data for $BaTiS_3$ nanocrystals (normalized and offset for clarity); reference $BaTiS_3$ pattern is shown along the bottom (black lines). Colors correspond to the legend shown in the top right. **(Right)** UV-Vis-NIR spectra (normalized and offset for clarity) of suspensions of the $BaTiS_3$ nanocrystals in tetrachloroethylene.

Barium dithiocarbamate compounds **1-4** were applied in the synthesis of colloidal $BaTiS_3$ nanorods in combination with a previously known titanium(IV) dithiocarbamate compound, $Ti(S_2CN^iPr_2)_4$ (**5**) as the $Ti^{4+}$ source.[30] In a standard reaction, the barium and titanium precursors are combined in a 2:1 molar ratio (excess $Ba^{2+}$) and dissolved in oleylamine at a concentration of 30 mM in [$Ba^{2+}$]; this was stirred at room temperature for 30 minutes, followed by heating to 350 °C under an atmosphere of dry nitrogen gas. Heating of the dark brown reaction solution was maintained for 30 minutes before the mixture was cooled to room temperature and the nanocrystals isolated by precipitation/centrifugation using toluene and ethanol (see the Supporting Information for further experimental details). We found that the use of at least a two-fold molar excess of the barium precursors was necessary to

give the desired product; at a 1:1 molar ratio, significant amounts of an impurity tentatively identified as $TiS_2$ or a similar compound are formed (see SI). No BaS by-products are isolated, suggesting that the excess barium is removed during the course of the workup. Consistent with that hypothesis, when barium dithiocarbamate compounds **1**-**4** are decomposed in oleylamine under the same conditions but in the absence of a titanium precursor, only very small amounts of BaS could be isolated as a by-product, and the resulting material was insoluble (non-colloidal).

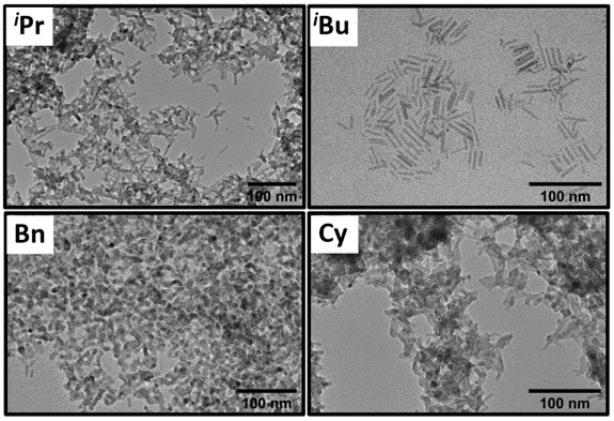


**Figure 4.** TEM images of $BaTiS_3$ nanocrystals synthesized using different precursors. The samples show varying degrees of aggregation during sample preparation.

Figure 3 shows characterization data (powder X-ray diffraction, PXRD, and UV-visible absorbance spectroscopy) for $BaTiS_3$ nanorods produced using the four different barium precursors **1**-**4**, while representative TEM data is shown in Figure 4. Characterization data for additional examples from each precursor are shown in the Supporting Information. The structural and spectroscopic properties of the $BaTiS_3$ nanorods synthesized using this method are generally consistent with those we recently reported using a different hot-injection approach involving metal amide precursors.[6] In particular, the particles show a similar rod-like morphology, with lengths of approximately 30 nm and average widths ranging from 6 to 8 nm (see SI for size distribution histograms for each sample). The powder XRD data shown in Figure 3 shows the reference pattern of bulk $BaTiS_3$ for comparison; the nanocrystal data show slight deviations from the bulk pattern, which are especially apparent in the position of the (002) diffraction peak at ~31.0°. This effect, which has been previously observed both in nanocrystals and in the solid state, is attributed to a sulfur deficiency in the material, which may be more accurately described as $BaTiS_\gamma$.[6,31] Like the previously synthesized nanomaterials, the UV-Vis-NIR absorbance spectra of these particles (Figure 3) shows a strong absorbance peak around 1600 nm whose exact energy varies from sample to sample; the source of this variability is still under investigation but does not seem to be correlated with particle size.

Our experiments have not revealed a clear correlation of the nanocrystal size, shape, structure, or spectral properties with the choice of barium dithiocarbamate precursor (compounds **1**-**4**). There is some sample-to-sample variation in nanocrystal properties (see SI), which may result from subtle changes in the reaction conditions such as heating rate, stirring speed, *etc.*; nanocrystal syntheses can be highly sensitive to such minor variations. Although the majority of reactions carried out under these standard conditions gave rise to nanorods similar to those shown in Figure 4, occasionally particles which were more irregular or poorly defined in shape were formed (see SI). The lack of a clear dependence on the nature of the substituents on the dithiocarbamate precursor is not surprising given the current understanding of the reaction pathways of dithiocarbamate ligands and complexes under similar conditions. Most likely, oleylamine exchanges into the dithiocarbamate ligands (transamination) to give monosubstituted ($R'HNCS_2^-$) dithiocarbamates which decompose more readily than the original disubstituted species in compounds **1**-**4**.[32] If decomposition of these oleylamine-exchanged dithiocarbamate ligands is primarily responsible for nanocrystal formation, then little dependence on the nature of the original disubstituted dithiocarbamate substituent is expected.

Compared to our previously reported hot-injection synthesis,[6] the current SSP method gives rise to materials with a smaller aspect ratio on average, and sometimes with a more irregular shape, at least under the standard conditions used here. While further optimization of this SSP method may improve the properties of the target nanomaterials, our preliminary opinion is that the hot-injection approach may be superior in terms of control afforded over the nanocrystal properties and the quality of the resulting materials. However, the SSP method using barium dithiocarbamates has the advantage of using a more straightforwardly synthesized and less air-sensitive $Ba^{2+}$ precursor, as well as the potential tunability of the precursor through facile variation of the dithiocarbamate substituents. While these substituents do not appear to have a strong impact on the reaction outcome under the conditions used here, they do affect the properties of the precursor, including its solubility; tunability at this site may be useful if these materials are applied in different processes such as thin-film preparation. Finally, the proof of principle for the use of the single-source barium precursors reported here provides an additional avenue of investigation towards the solution-phase synthesis of chalcogenide perovskite materials such as $BaZrS_3$, which have potential applications in thin-film photovoltaics.

This research is supported by the National Science Foundation through grant DMR-2004421. There are no conflicts to declare.

## Notes and references

1 A. Swarnkar, W. J. Mir, R. Chakraborty, M. Jagadeeswararao, T. Sheikh and A. Nag, *Chem. Mater.*, 2019, **31**, 565–575.

2 S. Niu, G. Joe, H. Zhao, Y. Zhou, T. Orvis, H. Huyan, J. Salman, K. Mahalingam, B. Urwin, J. Wu, Y. Liu, T. E. Tiwald, S. B. Cronin, B.

M. Howe, M. Mecklenburg, R. Haiges, D. J. Singh, H. Wang, M. A. Kats and J. Ravichandran, *Nat. Photonics*, 2018, **12**, 392–396.
3 B. Sun, S. Niu, R. P. Hermann, J. Moon, N. Shulumba, K. Page, B. Zhao, A. S. Thind, K. Mahalingam, J. Milam-Guerrero, R. Haiges, M. Mecklenburg, B. C. Melot, Y.-D. Jho, B. M. Howe, R. Mishra, A. Alatas, B. Winn, M. E. Manley, J. Ravichandran and A. J. Minnich, *Nat. Commun.*, 2020, **11**, 6039.
4 J. Wu, X. Cong, S. Niu, F. Liu, H. Zhao, Z. Du, J. Ravichandran, P.-H. Tan and H. Wang, *Adv. Mater.*, 2019, **31**, 1902118.
5 Jhon Cuya, Nobuaki Sato, Katsutoshi Yamamoto, Hideyuki Takahashi and Atsushi Muramatsu, *High Temp. Mater. Process.*, 2003, **22**, 197–202.
6 D. Zilevu and S. E. Creutz, *Chem. Mater.*, 2021, **33**, 5137–5146.
7 D. Tiwari, O. S. Hutter and G. Longo, *J. Phys. Energy*, 2021, **3**, 034010.
8 J. C. Sarker and G. Hogarth, *Chem. Rev.*, 2021, **121**, 6057–6123.
9 Y. Zhao, F. T. Rabouw, C. de M. Donegá, A. Meijerink and C. A. van Walree, *Mater. Lett.*, 2012, **80**, 75–77.
10 Y. Zhao, F. T. Rabouw, T. van Puffelen, C. A. van Walree, D. R. Gamelin, C. de Mello Donegá and A. Meijerink, *J. Am. Chem. Soc.*, 2014, **136**, 16533–16543.
11 P. S. Kubiak, A. L. Johnson, P. J. Cameron and G. Kociok-Köhn, *Eur. J. Inorg. Chem.*, 2019, **2019**, 3962–3969.
12 J. R. Thompson, PhD Thesis, University of Bath, 2017.
13 K. Ruhlandt-Senge and U. Englich, *Chem. – Eur. J.*, 2000, **6**, 4063–4070.
14 K. Naktode, T. D. N. Reddy, H. P. Nayek, B. S. Mallik, and T. K. Panda. *RSC Adv.,* 2015, **5**, 51413-51420.
15 A. Çetin and C. J. Ziegler, *Dalton Trans.*, 2006, 1006–1008.
16 J. Beck and Y. Ben-Amer, *Z. Für Anorg. Allg. Chem.*, 2007, **633**, 435–439.
17 I. K. Bezougli, A. Bashall, M. McPartlin and D. M. P. Mingos, *J. Chem. Soc. Dalton Trans.*, 1998, 2671–2678.
18 R. J. Butcher and A. P. Purdy, *Acta Crystallogr. Sect. E Struct. Rep. Online*, 2006, **62**, m342–m344.
19 M. Castillo, J. J. Criado, B. Macías and M. V. Vaquero, *Transit. Met. Chem.*, 1986, **11**, 476–479.
20 C. F. Conde, M. Millan, A. Conde and R. Márquez, *Acta Crystallogr. C*, 1986, **42**, 286–289.
21 A. S. A. Zidan, A. I. El-Said and A. A. M. Aly, *Synth. React. Inorg. Met.-Org. Chem.*, 1992, **22**, 1355–1362.
22 M. Castillo, A. Criado, R. Guzmán, J. J. Criado and B. Macias, *Transit. Met. Chem.*, 1987, **12**, 225–229.
23 W. Beck, M. Girnth, M. Castillo and H. Zippel, *Chem. Ber.*, 1978, **111**, 1246–1252.
24 A. Rai, S. K. Sengupta and O. P. Pandey, *Spectrochim. Acta. A. Mol. Biomol. Spectrosc.*, 2006, **64**, 789–794.
25 H. Siraj, K. S. Ahmad, S. B. Jaffri and M. Sohail, *Microelectron. Eng.*, 2020, **233**, 111400.
26 K. S. Ahmad, A. Zafar, S. B. Jaffri, M. K. Alamgir, M. Sohail, R. F. Mehmood, M. ur Rehman and D. Ali, *Results Phys.*, 2020, **19**, 103647.
27 A. P. Purdy and C. F. George, *Main Group Chem.*, 1996, **1**, 229–240.
28 A. F. Lindmark and R. C. Fay, *Inorg. Chem.*, 1983, **22**, 2000–2006.
29 R. M. Golding, P. C. Healy, P. W. G. Newman, E. Sinn and A. H. White, *Inorg. Chem.*, 1972, **11**, 2435–2440.
30 A. C. Behrle, A. J. Myers, A. Kerridge and J. R. Walensky, *Inorg. Chem.*, 2018, **57**, 10518–10524.
31 M. Saeki, M. Onoda and Y. Yajima, *J. Solid State Chem.*, 1996, **121**, 451–456.
32 N. Hollingsworth, A. Roffey, H.-U. Islam, M. Mercy, A. Roldan, W. Bras, M. Wolthers, C. R. A. Catlow, G. Sankar, G. Hogarth and N. H. de Leeuw, *Chem. Mater.*, 2014, **26**, 6281–6292.